

Realization of the purely spatial Einstein-Podolsky-Rosen paradox in full-field images of spontaneous parametric down conversion.

Paul-Antoine Moreau, Joé Mougin-Sisini, Fabrice Devaux, and Eric Lantz
Institut FEMTO-ST Département d'Optique PM Duffieux
UMR CNRS - Université de Franche-Comté n°6174,
Route de Gray 25030 Besançon Cedex, FRANCE
(Dated: November 29, 2019)

We present a demonstration of EPR entanglement by detecting purely spatial quantum correlations in the near and far-field of highly spatially multimode spontaneous parametric down conversion generated in a type 2 BBO crystal. Full field imaging is performed in the photon counting regime with an electron-multiplying CCD (EMCCD) camera. We obtain a violation of Heisenberg inequalities with inferred quantities taking into account all the biphoton pairs in both the near and far field.

PACS numbers: 03.65.Ud, 42.50.Dv, 42.50.Ar, 42.50.Lc

INTRODUCTION

In 1935, Einstein, Podolsky and Rosen (EPR) proposed a *gedanke experiment* [1] involving two spatially separated but entangled particles. They showed that quantum mechanics predicts that these particles could have both perfectly correlated positions and momenta, in contradiction with the so-called *local realism* where two distant particles should be treated as two different systems. Though the original intention of EPR was to show that quantum mechanics is not complete, the standard present view is that entangled particles do experience nonlocal correlations [2, 3].

Recently, the realization and detection of entangled EPR states aroused much interest of the scientific community following a testable formulation of the EPR paradox introduced by Reid [4], involving correlations of quadratures of twin beams. A recent review on the subject has been given in [5]. Furthermore, position and momentum entanglement of beams have been demonstrated at the EPR level by combining squeezed light from two spatial modes, with measurements by homodyne detection in the temporal domain [6, 7].

Spontaneous parametric down conversion (SPDC) provides independent pairs of entangled photons that makes the system very close of that considered in the original EPR paper: the positions of photons 1 and 2 are detected in the near-field and their momenta correspond to the far-field. Howell *et al.* [8] have measured in both planes the probability distribution of the position of photon 2, conditioned by the detection of photon 1. The product of the conditional variances was found to be 25 times smaller than the limit for the product of variances for a single photon given by the Heisenberg's uncertainty relation. This impressive result was obtained by measuring temporal coincidences between cross-polarized photons in type 2 SPDC. These photons were separated by a polarizing beam splitter: for a fixed position of a narrow slit transmitting the photon 1 to an avalanche photodiode,

the level of coincidences was measured for each position of a similar slit transmitting the photon 2 to a separate similar detector. Hence, in the words of Reid *et al.* [5]: "detection events are only considered if two emitted photons are simultaneously detected". In this sense, they did not prospect the full EPR characteristic of SPDC but a mono-dimensional and punctual EPR paradox using post selected data. The same comment could be made on the recent realization by Leach *et al.* [9], where the demonstration was punctual in one of the transverse dimensions of the field.

We present here a full spatial demonstration of EPR steering using highly spatially multimode type 2 SPDC. The use of type 2 phase matching allows us to spatially separate the idler and signal photons, so to be close of real conditions of an EPR test of local realism. By treating full-field bi-dimensional images of photo-detection without any data post selection, we assure a perfect correspondence between the system in the near and in far field [5], in contrast with punctual or 1-D detection. The detection is performed with an EMCCD camera. Their ability to reach the photon counting regime [10, 11] make them useful in quantum optics, and have already be used in our group to characterized quantum correlations in the far field of type 1 [12, 13] and type 2 [14] SPDC.

THEORY

SPDC induced by a wide monomode gaussian pump is a strongly multimode beam: the extension of the down converted beam in the near field (image plane) is identical to that of the pump, in the limit of low gain and for a sufficiently wide and thin crystal, while the far field (Fourier plane) extension is limited by phase-matching. The etendue of the beam, i.e. the product of its transverse surface by the solid angle it subtends or the number of transverse modes in appropriate units, corresponds to the two-photon Schmidt number [15].

The spatial extension of a mode in either the near or the far-field is proportional to the inverse of the full beam extension in the other plane. For single photon imaging, the laws of diffraction are equivalent to the Heisenberg's uncertainty relation: a photon that can be localized in one mode of the near field, for example by traversing an aperture of the size corresponding to the mode, will be detected at a random position in the entire far-field diffraction pattern. However, the laws of quantum mechanics state that a pair of signal-idler photons will be detected either in the same mode in the near field or in opposite modes in the far field, if no detection occurs in the other plane. Because the detection plane can be chosen at a time where causal interaction between photons is no more possible, these correlations are not compatible with local realism, as demonstrated first in the EPR paper [1], though compatible with the Heisenberg's uncertainty relation since correlations cannot be measured in both planes for the same photon pair.

We can describe the SPDC behavior as follows: for a detection of a photon 1 at \mathbf{r}_1 , the probability density of detection of a photon 2 at \mathbf{r}_2 can be written as:

$$p(\mathbf{r}_2 | \mathbf{r}_1) = p(\mathbf{r}_2) + f(\Delta\mathbf{r}) \quad (1)$$

where $p(\mathbf{r}_2)$ is the probability density of detection of a photon of another pair (accidental coincidences) and $f(\Delta\mathbf{r})$ is the probability density of detection of the twin photon, with $\Delta\mathbf{r} = \|\mathbf{r}_2 \pm \mathbf{r}_1\|$, + holding for the far-field (correlation of momenta on opposite modes) and - for the near-field. It is assumed translational invariance, circular symmetry and independence of the pairs (pure SPDC without further amplification). Hence, if N_1 is the number of photons 1 detected on a surface S_1 and N_2 the corresponding quantity for photons 2, we have:

$$\begin{aligned} \langle N_1 N_2 \rangle &= \int_{S_1} d^2\mathbf{r}_1 \int_{S_2} d^2\mathbf{r}_2 p(\mathbf{r}_1, \mathbf{r}_2) \\ &= \int_{S_1} d^2\mathbf{r}_1 \int_{S_2} d^2\mathbf{r}_2 \{p(\mathbf{r}_1)p(\mathbf{r}_2) + p(\mathbf{r}_1)f(\Delta\mathbf{r})\} \end{aligned} \quad (2)$$

Therefore, the probability of detection in S_2 of the twin photon 2 of the photon 1 detected on S_1 is simply given by:

$$F(S_2) = \int_{S_2} d^2\mathbf{r}_2 f(\Delta\mathbf{r}) = \frac{\langle N_1 N_2 \rangle - \langle N_1 \rangle \langle N_2 \rangle}{\langle N_1 \rangle} \quad (3)$$

If S_1 and S_2 have the same size, this expression can be symmetrized and becomes the normalized intercorrelation function:

$$F(S_2) = F(S_1) = \frac{\langle N_1 N_2 \rangle - \langle N_1 \rangle \langle N_2 \rangle}{\frac{1}{2}(\langle N_1 \rangle + \langle N_2 \rangle)} \quad (4)$$

The mean in this equation can be estimated by spatial averages on the different pixels of the image for a fixed $\Delta\mathbf{r}$, given by the intercorrelation of two "regions of interest" (ROIs) of an image, each one corresponding to one

polarization of the SPDC. We will therefore obtain a non local estimation involving all the light. Note that deterministic spatial variations of the mean intensity do not preclude the validity of these spatial averages, inasmuch as the width of the intercorrelation function is smaller than the scale of this deterministic variation. Indeed, the covariance signal-idler for a region formed by independent area is the sum of the covariances of each area, just as the mean for the region is the sum of the means for each area. Hence, if the ratio between the covariance and the mean intensity does not depend of this mean, it will be retrieved by spatial averaging even if the mean varies spatially. Because of the weak signal to noise ratio, we proceed to an additional statistical average on different images taken at different times for the same system configuration.

For independent pairs, the quantity in equation (4) can be expressed as a function of the variance of the difference between N_1 and N_2 :

$$\begin{aligned} \langle N_1 \rangle &= \langle N_2 \rangle = \langle N_1^2 \rangle - \langle N_1 \rangle^2 \\ \Rightarrow F(S_2) &= 1 - \frac{\langle (N_1 - N_2)^2 \rangle}{\langle N_1 + N_2 \rangle} \end{aligned} \quad (5)$$

The physical quantities used to test the EPR violation of Heisenberg inequalities are the spatial variances in each dimension σ_x^2 and σ_y^2 . To define an unique global criterion, we use the mean value of the two variances (i.e. half of the mean of the squared distance) :

$$\sigma_{r,k}^2 = \frac{\sigma_{x,k_x}^2 + \sigma_{y,k_y}^2}{2} \quad (6)$$

Thus, by introducing the Heisenberg inequalities in the near-field far-field products one gets:

$$\sigma_r^2 \sigma_k^2 = \frac{1}{4}(\sigma_x^2 + \sigma_y^2)(\sigma_{k_x}^2 + \sigma_{k_y}^2) \geq \frac{\hbar^2}{4} \quad (7)$$

We have used the fact that $\sigma_x^2 \sigma_{k_x}^2 + \sigma_y^2 \sigma_{k_y}^2 \geq 2\frac{\hbar^2}{4}$. Note that this two dimensional diffraction limit will only be reached by isotropic 2-D gaussians.

EXPERIMENT

The experimental setup is represented in Fig. 1. The pump pulse at 355 nm provided by a passively Q-switch Nd:YAG laser (mean power: 27 mW, pulse duration: 300 ps, repetition rate: 1 kHz), illuminates a 1 mm long type 2 BBO nonlinear crystal. The far-field image of the SPDC is formed on the EMCCD in the focal plane of a 37 mm focal aspheric lens: Fig. 1(a). In the near field configuration, Fig 1(b), the signal and idler photons are separated by a Wollaston prism of 1.5 of angular separation positioned around the Fourier plane. The plane in the middle of the BBO crystal is imaged on the

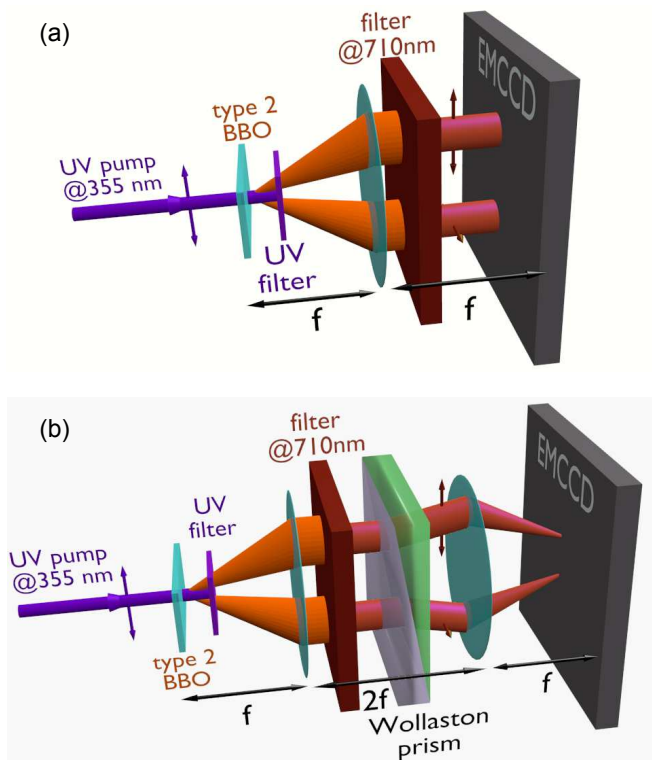


FIG. 1. Experimental setups. (a) Far field. (b) Near field.

EMCCD plane by a second identical aspheric lens, in order to minimize the walk-off effects [16]. The transversal magnification has been checked: $\gamma = 1.003 \pm 0.005$. The back-illuminated EMCCD camera from Andor Technology (Model iXon+ DU897-ECS-BV) has a quantum efficiency greater than 90% in the visible range. The detector area is formed by 512×512 pixels, with a pixel size of $s_{pix} = 16 \times 16 \mu\text{m}^2$ (i.e. $0.46 \times 0.46 \text{ mrad}^2$ in the far field after division by the focal length). We used a read-out rate of 10 MHz at 14 bits and the camera was cooled to -85°C . Measurements were performed for a crystal orientation corresponding to collinear phase matching at degeneracy. Photon pairs emitted around the degeneracy are selected by mean of a narrow-band interference filter centered at 710 nm ($\Delta\lambda=4 \text{ nm}$). As in [13] and [14], photon counting regime is ensured by adjusting the exposure time in such a way that the mean fluence of SPDC was between 0.1 and 0.2 photon per pixel. Moreover, the use of pump pulses with 300 ps duration (much longer than the coherence time of SPDC) and an exposure time of the EMCCD of 10 ms (i.e. 10 laser shots) allow the excess noise to be limited by increasing the number of temporal modes [17]: the mean number of photons for one spatiotemporal mode is less than 10^{-3} , in good agreement with the hypothesis of pure spontaneous parametric down conversion, without any stimulated amplification.

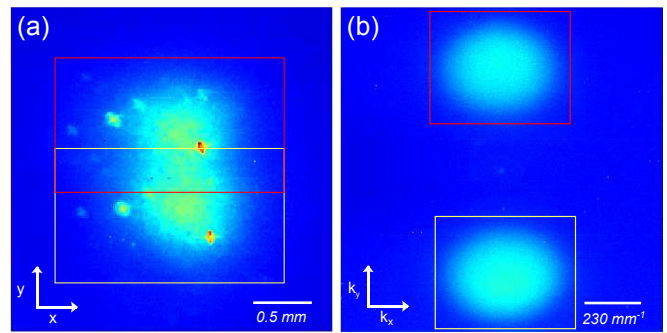


FIG. 2. Intensity distributions. (a) Near field. (b) Far field. In both figures rectangles denote the ROIs used for calculation.

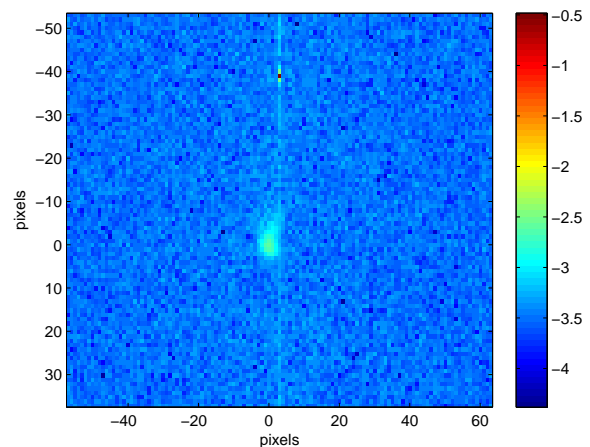


FIG. 3. Near-field complete intercorrelation in log scale.

NEAR FIELD

We show in Fig. 2 (a) the sum of the 10000 near field images. The two SPDC patterns are clearly visible, with inhomogeneities and hot spots due to defaults on the crystal. The ROIs corresponding to either the signal or the idler, large enough to encompass all the light for each polarization, have a common area. As a consequence, the intercorrelation function exhibits a strong autocorrelation peak, as it can be seen on Fig. 3, but the intercorrelation peak, due to quantum correlations, and the autocorrelation peak are clearly distinguishable. We use a Fourier algorithm without any zero padding to compute the intercorrelation, which is equivalent to a periodisation of the images. In the Fig. 4 are presented the near-field intercorrelation peak obtained from ROIs taken in the same image and a witness intercorrelation obtained from ROIs taken in two successive images. The absence of any non-negligible intercorrelation value in the second image shows that the inhomogeneities in the crystal do not create any deterministic intercorrelation pattern. The first image exhibits a weak intercorrelation vertical line,

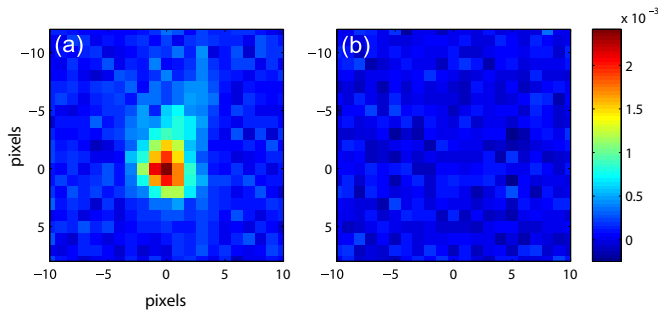


FIG. 4. (a) Near-field intercorrelation function. (b) Corresponding witness intercorrelation.

more visible in Fig. 3 because of the log scale, which is due to the spreading of the autocorrelation peak induced by smearing in the gain register of the EMCCD camera. It again shows the importance to sufficiently separate the signal and idler photons on the camera to avoid any superposition of the autocorrelation and intercorrelation peaks. By fitting the intercorrelation peak with a two dimensional gaussian function, we estimate the inferred near-field standard deviations in pixels:

$$\sigma_x = 1.53 \pm 0.07, \quad \sigma_y = 2.2 \pm 0.1, \quad \sigma_r = 1.89 \pm 0.09 \quad (8)$$

By integrating the fitted curve, we also obtain the total quantum correlation coefficient in the near field: $R_n = 5 \cdot 10^{-2}$.

FAR FIELD

In the Fig. 2 (b) is shown the sum of 10000 images in the far-field configuration. The intercorrelation function obtained in the far-field is presented in Fig. 5. Note that the anisotropy of the peak is mainly due to the anisotropy of the shape of the pump. However, as predicted by simulations, an enlargement exists due to the non perfect degeneracy of the photons wavelength. This enlargement is itself anisotropic and, as predicted by the theory, is greater in the walk-off direction which separate the two fluorescence spots in the far field (vertical direction on each image presented here). The experimental results are in agreement with this phenomenon since the enlargement of the intercorrelation peak is greater in the vertical dimension than in the horizontal one [14]. We finally find the inferred standard deviations in far-field pixel units:

$$\sigma_{k_x} = 2.35 \pm 0.08, \quad \sigma_{k_y} = 1.85 \pm 0.07, \quad \sigma_k = 2.11 \pm 0.7 \quad (9)$$

The total quantum correlation coefficient in the far field is $R_k = 4.4 \cdot 10^{-2}$. In agreement with Eq. 5, we have experimentally shown in [14] that $(1 - R_k)$ is equal to the variance of the difference between areas greater than the coherence cell, expressed in shot noise units.

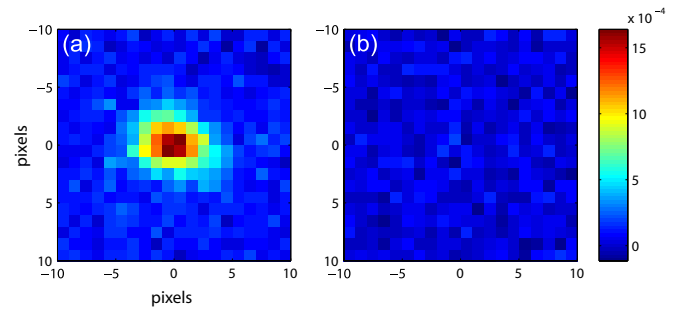


FIG. 5. (a) Far-field intercorrelation function. (b) Corresponding witness intercorrelation.

EPR VIOLATION OF THE HEISENBERG INEQUALITIES

We are now able to test the violation of the Heisenberg inequalities by using the inferred quantities we have measured. In the horizontal direction, we have:

$$\begin{aligned} \sigma_x^2 \sigma_{k_x}^2 &= \left(1.53 \times 2.35 \frac{2\pi \cdot s_{pix} \hbar}{f \cdot \lambda} \right)^2 \\ &= (0.048 \pm 0.008) \hbar^2 < \frac{\hbar^2}{4} \end{aligned} \quad (10)$$

giving a violation factor of 5.2 ± 0.8 .

In the vertical direction, we find:

$$\sigma_y^2 \sigma_{k_y}^2 = (0.06 \pm 0.01) \hbar^2 < \frac{\hbar^2}{4} \quad (11)$$

giving a violation factor of 4 ± 1 .

And finally, by using the complete statistic of the fluorescence, from (6) and (7) one obtain:

$$\sigma_r^2 \sigma_k^2 = (0.06 \pm 0.01) \hbar^2 < \frac{\hbar^2}{4} \quad (12)$$

which gives a violation factor of 4 ± 1 .

CONCLUSION

We have demonstrated a purely spatial EPR paradox by using a full field and direct detection method. The violation of the Heisenberg inequalities for the inferred quantities has been demonstrated for both transverse dimensions, by recording all the photon pairs generated by spontaneous parametric down conversion in the near field and the far field of the same system.

Some of the computations have been performed on the supercomputer facilities of the Mésocentre de calcul de Franche-Comté.

[1] A. Einstein, B. Podolsky, and N. Rosen, Phys. Rev. **47**, 777 (1935).

- [2] J. S. Bell, *Physics* **1**, 195 (1964).
- [3] A. Aspect, P. Grangier, and G. Roger, *Phys. Rev. Lett.* **47**, 460 (1981).
- [4] M. D. Reid, *Phys. Rev. A* **40**, 913 (1989).
- [5] M. D. Reid, P. D. Drummond, W. P. Bowen, E. G. Cavalcanti, P. K. Lam, H. A. Bachor, U. L. Andersen, and G. Leuchs, *Rev. Mod. Phys.* **81**, 1727 (2009).
- [6] K. Wagner, J. Janousek, V. Delaubert, H. Zou, C. Harb, N. Treps, J. F. Morizur, P. K. Lam, and H. A. Bachor, *Science* **321**, 541 (2008).
- [7] V. Boyer, A. M. Marino, R. C. Pooser, and P. D. Lett, *Science* **321**, 544 (2008).
- [8] J. C. Howell, R. S. Bennink, S. J. Bentley, and R. W. Boyd, *Phys. Rev. Lett.* **92**, 210403 (2004).
- [9] J. Leach, R. E. Warburton, D. G. Ireland, F. Izdebski, S. M. Barnett, A. M. Yao, G. S. Buller, and M. J. Padgett, *Phys. Rev. A* **85**, 013827 (2012).
- [10] E. Lantz, J.-L. Blanchet, L. Furfaro, and F. Devaux, *Monthly Notices Of The Royal Astronomical Society* **386**, 2262 (2008).
- [11] O. Jedrkiewicz, J.-L. Blanchet, E. Lantz, and P. D. Trapani, *Optics Communications* **285**, 218 (2012).
- [12] J.-L. Blanchet, F. Devaux, L. Furfaro, and E. Lantz, *Phys. Rev. Lett.* **101**, 233604 (2008).
- [13] J.-L. Blanchet, F. Devaux, L. Furfaro, and E. Lantz, *Phys. Rev. A* **81**, 043825 (2010).
- [14] F. Devaux, J. Mougin-Sisini, P.-A. Moreau, and E. Lantz, *Submitted* (2012).
- [15] M. P. van Exter, A. Aiello, S. S. R. Oemrawsingh, G. Nienhuis, and J. P. Woerdman, *Phys. Rev. A* **74**, 012309 (2006).
- [16] E. Brambilla, A. Gatti, M. Bache, and L. A. Lugiato, *Phys. Rev. A* **69**, 023802 (2004).
- [17] E. Brambilla, L. Caspani, O. Jedrkiewicz, L. A. Lugiato, and A. Gatti, *Phys. Rev. A* **77**, 053807 (2008).